Decomposition of LiGdF$_4$ scheelite at high pressures

Andrzej Grzechnik[1,7]**, Wilson A Crichton**[2]**, Pierre Bouvier**[3]**,
Vladimir Dmitriev**[4]**, Hans-Peter Weber**[4,5] **and Jean-Yves Gesland**[6]

[1] Departamento de Física de la Materia Condensada, Universidad del País Vasco, Apartado 644,
Bilbao, E-48080, Spain
[2] European Synchrotron Radiation Facility, BP 220, F-38043 Grenoble cedex, France
[3] Laboratoire d'Electrochimie et de Physicochimie des Materiaux et des Interfaces (LEPMI),
UMR 5631-CNRS, 1130 Rue de la Piscine, BP 75, F-38402 Saint Martin d'Heres cedex, France
[4] Group 'Structure of Materials under Extreme Conditions', Swiss–Norwegian Beamlines,
European Synchrotron Radiation Facility, BP 220, F-38043 Grenoble cedex, France
[5] Laboratoire de Cristallographie, EPFL/SB/IPMC/LCR, École Polytechnique Fédéral de
Lausanne, CH-1015 Lausanne, Switzerland
[6] Université du Maine-Cristallogenese, F-72025 Le Mans cedex, France

E-mail: andrzej@wm.lc.ehu.es

Abstract
The high-pressure behaviour of LiGdF$_4$ scheelite ($I4_1/a$, $Z = 4$) was studied
by measuring its angle-dispersive x-ray powder diffraction patterns as a function
of pressure and temperature in a diamond anvil cell and a large-volume Paris–
Edinburgh cell using a synchrotron radiation source. Upon compression to
about 11 GPa at room temperature, the stable structure is of the scheelite
type. At higher pressures and $T = 298$ K, new reflections occur that cannot
be explained with the fergusonite structural model previously observed for
LiYF$_4$. Associated with this is the growth of an amorphous component. All the
transformations are largely irreversible upon decompression. Annealing of the
sample at 13.1 GPa led to a nucleation of a solid solution series Li$_y$Gd$_{1-y}$F$_{3-2y}$
($P6_3/mmc$, $Z = 2$) and traces of LiF. The new material Li$_y$Gd$_{1-y}$F$_{3-2y}$
($P6_3/mmc$, $Z = 2$) was recovered to ambient conditions but back-transformed
to a YF$_3$-type phase ($Pnma$, $Z = 4$) after regrinding at room temperature for
several hours. These observations are discussed in relation to the high-pressure
high-temperature systematics of the AMX$_4$-type compounds.

1. Introduction

Fluoride compounds of the form LiMF$_4$, where M is a trivalent cation, have the CaWO$_4$-type
or scheelite-type structure ($I4_1/a$, $Z = 4$), which is a superstructure of fluorite CaF$_2$ ($Fm\overline{3}m$,

---

[7] Author to whom any correspondence should be addressed.

$Z = 4$). The fluorine atoms are in a distorted simple cubic arrangement and the Li^{1+} and M^{3+} cations are fourfold and eightfold coordinated by fluorines, respectively. When M is a lanthanide atom or yttrium, these compounds are scintillators, laser hosts, and luminescence materials [1].

It has recently been reported that $LiYF_4$ scheelite transforms to a fergusonite-type structure ($I2/a$, $Z = 4$) at about 10 GPa [2]. The transition involves small distortions of the cationic matrix and significant displacements of the anions. Like scheelite, fergusonite is an ordered superstructure of the fluorite type. The crystal structure of an additional polymorph of $LiYF_4$, stable above about 17 GPa, has not been solved yet. Other crystallographic information on the high-pressure behaviour of fluoride scheelites is not available in the literature. Molecular dynamics simulation of pressure-induced phase transitions in $LiYF_4$ and $LiYbF_4$ has predicted that their post-scheelite (post-fergusonite) polymorphs would be structurally related to the $LaTaO_4$ type ($P2_1/c$, $Z = 4$), with the Li^{1+} and Y^{3+} cations octahedrally and tenfold coordinated to the fluorine atoms, respectively [3]. From the comparison of the total energy differences for the $BaWO_4$-II type ($P2_1/n$, $Z = 8$), $LaTaO_4$ type ($P2_1/c$, $Z = 4$), $BaMnF_4$ type ($Cmc2_1$, $Z = 4$), and $NiWO_4$ wolframite type ($P2/c$, $Z = 2$) using electronic structure calculations, Li *et al* have concluded that the post-fergusonite structure of $LiYF_4$ is wolframite, an ordered superstructure of α-PbO_2 ($Pbcn$, $Z = 4$), with all the cations octahedrally coordinated to fluorines [4]. However, in the high-pressure study on $CaWO_4$ [5], it has been demonstrated that the transformation scheelite $\rightarrow$ wolframite, for all AMX_4 compounds, is not to be expected on the basis of the high-pressure high-temperature systematics in the AX_2 group of materials since the rutile-type AX_2 phases transform towards the fluorite type at high pressures, with the α-PbO_2-type structure as one of the possible intermediates in the process [6, 7].

Considering all the discrepancies in the literature, one could conclude that pressure-induced post-scheelite (or post-fergusonite) structures in oxides, fluorides, and any other AMX_4-type compounds are not really well known. Further experimental investigations to find pressure-induced post-scheelite structures are thus warranted. This study aims to elucidate the high-pressure behaviour of $LiGdF_4$ by measuring its angle-dispersive x-ray powder diffraction patterns as a function of pressure and temperature using a synchrotron source.

2. Experimental details

Angle-dispersive powder x-ray diffraction patterns in a diamond anvil cell (using a methanol:ethanol mixture as a pressure medium) were measured at room temperature on the Swiss–Norwegian Beamlines at the European Synchrotron Radiation Facility (BM1A, ESRF, Grenoble, France). Monochromatic radiation at 0.7100 Å was used for data collection on the image plate (MAR345). The images were integrated using the program FIT2D [8] to yield diagrams of intensity versus 2θ. The ruby luminescence method [9] was used for pressure measurements.

Angle-dispersive x-ray powder diffraction experiments ($\lambda = 0.158\,16$ Å) at high pressures and high temperatures were carried out using the large-volume Paris–Edinburgh facility at the ID30 Beamline of the European Synchrotron Radiation Facility, Grenoble, France. The sample was loaded into a hexagonal BN capsule with an 0.8 mm internal diameter. Together with a graphite furnace, it was embedded in a boron–epoxy gasket. A multi-slit system was employed during the experiment, which allows sample diffraction patterns to be taken with a minimum of signal from the capsule, surrounding furnace, and B–epoxy gasket. Pressures and temperatures were estimated from known fusion curves and an internal cross-calibration method based on the position of diffraction peaks due to boron nitride and gold internal
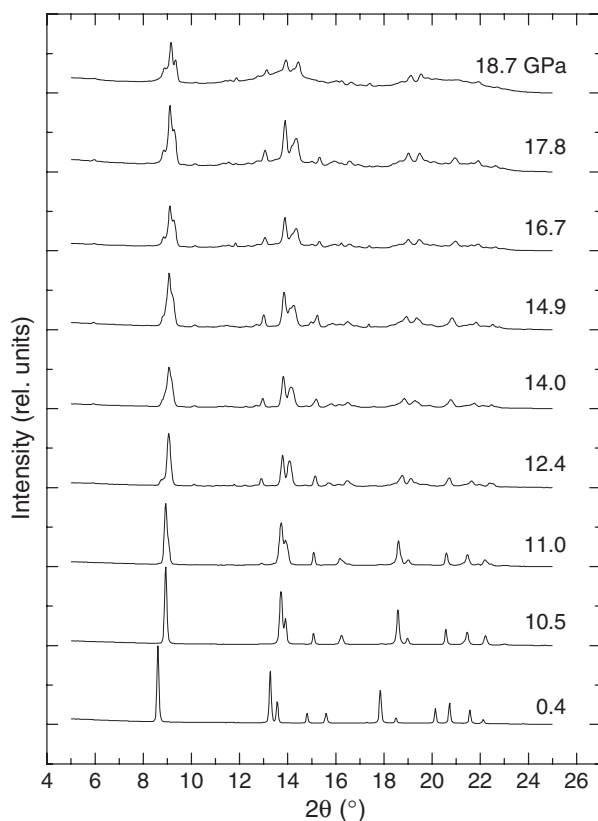
Figure 1. Selected x-ray powder patterns collected in a diamond anvil cell at different pressures upon compression at room temperature; $\lambda = 0.7100$ Å (Swiss–Norwegian Beamlines, ESRF).

standards [10]. The maximum error in pressures was evaluated to be 0.1 GPa. The relative errors in temperatures do not exceed 10%. Two-dimensional images were recorded using a MAR345 image plate detector and were integrated using the program FIT2D [8] to yield diagrams of intensity versus 2θ.

In all the experiments carried out for this study, wavelengths were stable over the time of the measurements (as a whole) and were compared by rechecking the distance between the detectors and samples (with the wavelengths and calibrated sample d-spacings fixed).

3. Results

Diffraction patterns of LiGdF$_4$ collected in a diamond anvil cell at different pressures and room temperature (Swiss–Norwegian Beamlines, ESRF) are shown in figures 1 and 2. Upon compression to about 11 GPa, the stable structure is of the scheelite type ($I4_1/a$, $Z = 4$). At higher pressures (figure 1), new reflections occur that cannot be accounted for with the fergusonite structure previously observed in LiYF$_4$ [5]. Associated with this is the growth of an amorphous component as seen from the emergence of broad features in the patterns. Upon decompression, the amorphous background is observed down to atmospheric pressure while the remaining crystalline LiGdF$_4$ transforms back to the scheelite structure (figure 2).

Figure 3 shows the pressure dependence of the lattice parameters, unit-cell volumes, and axial ratios for the scheelite polymorph of LiGdF$_4$ to about 11 GPa. The lattice parameters at ambient pressure are $a = 5.235(1)$ Å, $c = 11.019(2)$ Å, $V = 302.0$ Å^3. The compression data could be fitted by a Birch–Murnaghan equation of state, giving the zero-pressure bulk modulus
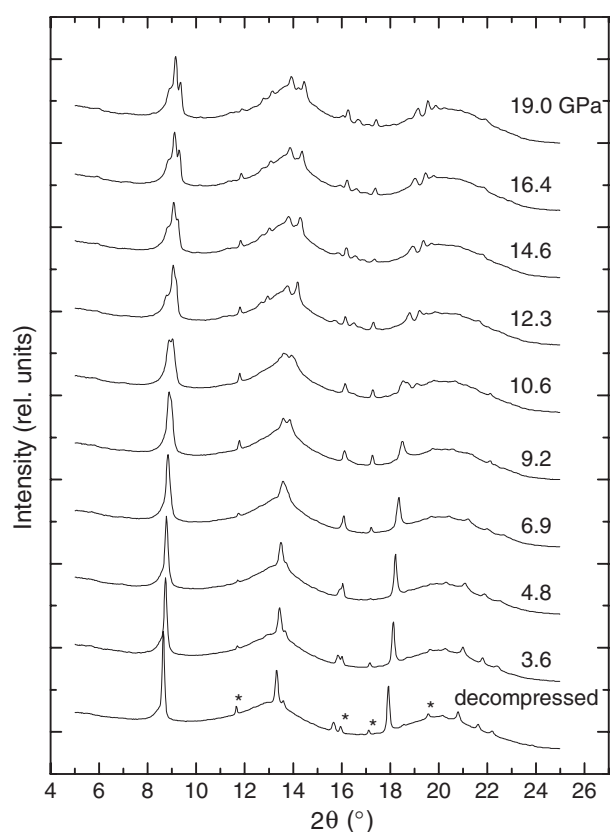
Figure 2. Selected x-ray powder patterns collected in a diamond anvil cell at different pressures upon decompression at room temperature; $\lambda = 0.7100$ Å (Swiss–Norwegian Beamlines, ESRF). Stars indicate reflections due to Cr-doped Al_2O_3 (ruby) used as a pressure calibrant.

$B_0 = 76 \pm 4$ GPa, the first pressure derivative of the bulk modulus $B' = 5.01 \pm 1.03$, and the unit-cell volume of scheelite at ambient pressure $V_0 = 302.9 \pm 0.3$ Å^3. These values could be compared with those for LiYF$_4$ [5]: $B_0 = 81 \pm 4$ GPa, $B' = 4.97 \pm 0.68$, $V_0 = 285.1 \pm 0.5$ Å^3. The c/a axial ratios are a measure of the tetragonal distortion of the fluorite superstructure, the ideal value being equal to 2 [6, 11]. Like for LiYF$_4$ [5], the c/a ratios in LiGdF$_4$ scheelite increase upon compression, indicating that the distortions in both materials are enhanced at high pressures.

In situ high-pressure and high-temperature measurements were performed using the large-volume Paris–Edinburgh facility at the ID30 Beamline of the European Synchrotron Radiation Facility. The sample was compressed to about 13 GPa and annealed at different temperatures to crystallize the amorphous phase (figure 4). Annealing at 13.1 GPa and 500 K led to a nucleation of a new material that at higher temperatures was almost completely crystallized, while the scheelite form of LiGdF$_4$ was a minor component. The new material was recovered to ambient conditions but back-transformed to another phase after regrinding at room temperature for several hours (figure 5).

The x-ray powder pattern of the sample recovered to atmospheric pressure collected immediately after the experiment (figure 5) was indexed using the program DICVOL91 [12] with a hexagonal unit cell: $a = 3.9850(9)$ Å, $c = 7.081(2)$ Å, $V = 97.39$ Å^3, $M(20) = 37.8$, $F(20) = 281.1$ (0.0026, 27). The systematic absences indicated that the space group is $P6_3/mmc$ or $P\overline{3}1c$ [13]. The lattice parameters agreed very well with the parameters for the tysonite type ($P6_3/mmc$, $Z = 2$) [14]. Indeed, the pattern of pure GdF$_3$ [15] calculated using
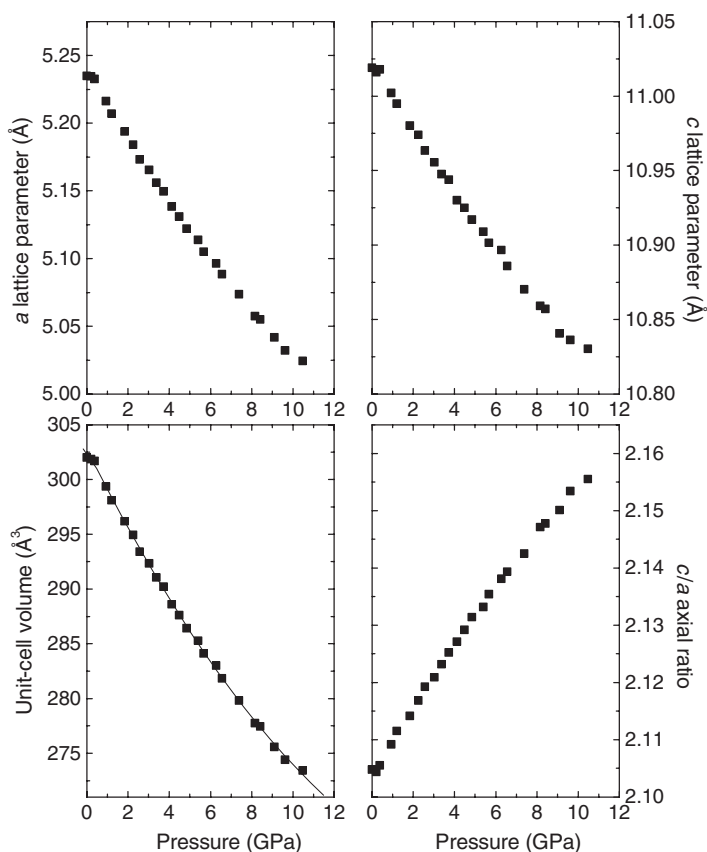
Figure 3. The pressure dependence of the lattice parameters, unit-cell volumes, and axial ratios for the scheelite polymorph ($I4_1/a$, $Z = 4$). The solid curve represents the Birch–Murnaghan equation of state.

the structural model for tysonite [14] almost perfectly matched the observed one. On the other hand, the pattern recorded several hours after the experiment could be approximated as that of a mixture of the tysonite ($P6_3/mmc$, $Z = 2$) and YF$_3$ ($Pnma$, $Z = 4$) [16, 17] structure types of pure GdF$_3$, e.g., see the (011) reflection of tysonite (figure 5).

4. Discussion

At ambient conditions, the trifluorides of rare earths from Sm to Lu crystallize in the YF$_3$ structure ($Pnma$, $Z = 4$) with the cations ninefold coordinated to fluorines [16, 17]. Lanthanide trifluorides from La to Nd have the structure of fluocerite ($P\bar{3}c1$, $Z = 6$), in which, depending on the interpretation of interatomic distances, lanthanides are ninefold or elevenfold coordinated to fluorines [16, 18]. Mixed lanthanide trifluorides, such as (La, Ce, . . .)F$_3$, are tysonites [16]. According to generalized P–T phase diagrams for transition metal trifluorides [17, 19], one should expect the $Pnma \rightarrow P\bar{3}c1$ phase transition for LnF$_3$ (Ln:Sm–Lu) at high pressures. The high-pressure forms of LaF$_3$ and CeF$_3$ ($Cmma$, $Z = 8$) are distorted modifications of hypothetical fluorite-like trifluoride [20]. At atmospheric conditions, the tysonite or fluocerite structures allow non-stoichiometric solid solutions and composites in the systems LiF–RF$_3$ [21] and NaF–RF$_3$ [22] (R = rare earth element). The LiF–GdF$_3$ phase
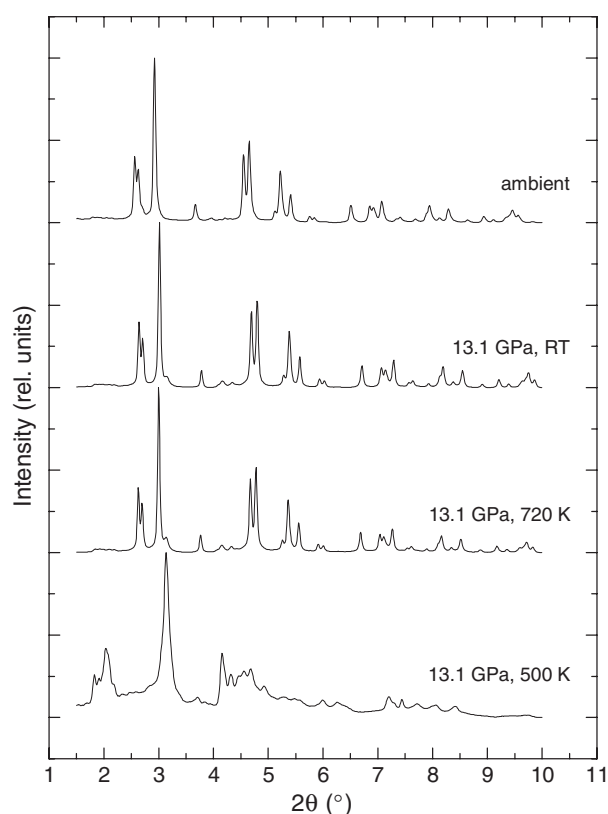
Figure 4. Selected x-ray powder patterns collected in a large-volume Paris–Edinburgh cell at different pressures and temperatures; $\lambda = 0.158\,16$ Å (ID30 Beamline, ESRF).

diagram has two invariant points: a eutectic at 25 mol% GdF_3 and 973 K as well as a peritectic at 34 mol% GdF_3 and 1023 K [23]. $LiGdF_4$ (50 mol% GdF_3) itself has a strong incongruent melting behaviour.

The data presented in figures 4 and 5, in which the x-ray powder patterns of the sample recovered to ambient conditions from high pressures and high temperatures could be well explained with calculated diagrams assuming the tysonite or YF_3 structural models for pure GdF_3, provide evidence for a pressure-induced decomposition of $LiGdF_4$ scheelite. Although our data do not give any hint on the exact chemical composition of the dissociation products, the most probable formula of the components is the tysonite-like phase as a solid solution $Li_yGd_{1-y}F_{3-2y}$ and LiF; see the weak (111) reflection of LiF at 3.9° (figures 4 and 5). A similar solid solution based on lanthanide trifluorides has been found in the $NaF–RF_3$ (R = rare earth element) systems at atmospheric pressure [22]. In fact, substituting lithium and varying fluorine occupancies in the tysonite structural model have a very weak effect on the calculated x-ray powder diffraction intensities [15]. It is interesting to note that the x-ray powder patterns of $LiGdF_4$ collected above 11 GPa at room temperature have broad features that are due to an amorphous phase (figure 1). The formation of the amorphous component is irreversible (figure 2). Thus, all our data indicate that the pressure-induced amorphization of $LiGdF_4$ scheelite is in fact due to its chemical decomposition, the process recently found in several other compounds under compression [24–26]. The decomposition and amorphization processes are linked to coordination changes around the cations, and especially around the Gd^{3+} cations, which in the tysonite-type compound $Li_yGd_{1-y}F_{3-2y}$ are ninefold or elevenfold coordinated to fluorines [16, 18].
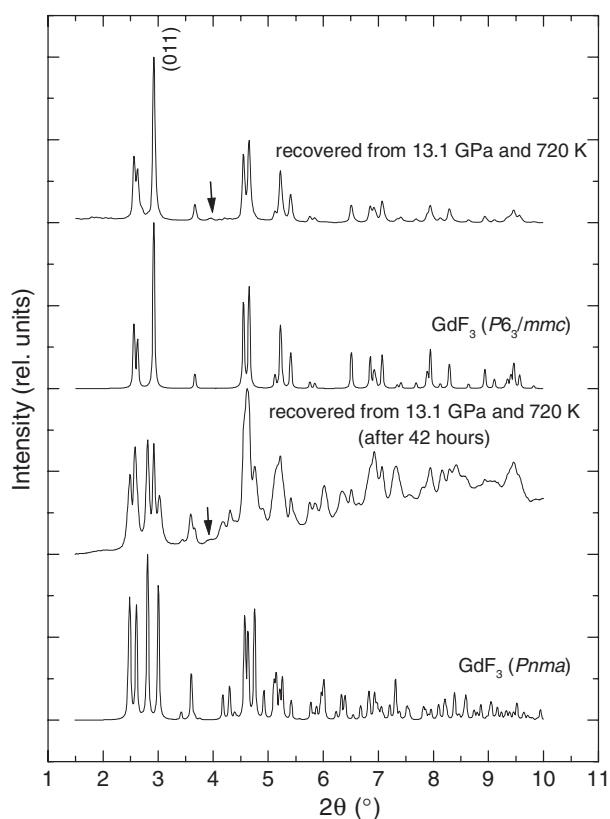
Figure 5. Comparison of measured patterns for the recovered sample immediately after the experiment and after 42 h (ID30 Beamline, ESRF) with calculated patterns [15] for pure GdF$_3$ in the tysonite ($P6_3/mmc$, $Z = 2$, $a = 3.985(1)$ Å, $c = 7.081(2)$ Å) and β-YF$_3$ ($Pnma$, $Z = 4$, $a = 6.696(2)$ Å, $b = 6.962(2)$ Å, $c = 4.342(1)$ Å) structures; $\lambda = 0.158\,16$ Å. The (011) reflection in the tysonite type is marked. The arrows indicate the (111) reflection due to LiF.

Our observation that LiGdF$_4$ scheelite decomposes at high pressures is very similar to the behaviour of some silicate zircons and monazites, both closely related to the rutile TiO$_2$ type ($P4_2/mnm$, $Z = 2$), that under compression firstly forms scheelites and then, in several cases, dissociates to component oxides [27]. For instance, ZrSiO$_4$ scheelite directly decomposes to ZrO$_2$ cotunnite ($Pnam$, $Z = 4$) and SiO$_2$ stishovite ($P4_2/mnm$, $Z = 2$) with the phase boundary between ZrSiO$_4$ and the ZrO$_2$ + SiO$_2$ composite having a positive Clapeyron slope. This behaviour is in contrast with that of zircon-like sulfates and selenates stable in post-barite (scheelite) conditions since silicate zircons could in fact be considered as double oxides, while zircon-like sulfates and selenates are salts [28]. Work is in progress to investigate the behaviour of sulfate and silicate phases with the aim of finding out the crystal-chemical reason for this divergence at high pressures [28]. The results of our study on LiGdF$_4$ clearly demonstrate that additionally to scheelite phase transformations into the BaWO$_4$-II ($P2_1/n$, $Z = 8$), LaTaO$_4$ ($P2_1/c$, $Z = 4$), or BaMnF$_4$ ($Cmc2_1$, $Z = 4$) types [2–5, 29], a decomposition of fluoride scheelites has to be considered in order to establish the high-pressure high-temperature systematics of the AMX$_4$ type compounds. In particular, the behaviour of scheelite structured fluorides differing in the rare earth metal as well as in their structural relationship with LiYF$_4$ should be further investigated.

5. Conclusions

The results of high-pressure high-temperature investigations on LiGdF$_4$ scheelite ($I4_1/a$, $Z = 4$) using synchrotron angle-dispersive x-ray powder diffraction show that above 11 GPa it progressively decomposes into a solid solution series Li$_y$Gd$_{1-y}$F$_{3-2y}$ ($P6_3/mmc$, $Z = 2$) and LiF.

Acknowledgments

References

[1] Burkhalter R, Dohnke I and Hulliger J 2001 *Prog. Crystallogr. Growth Charact.* **42** 1
   Braud A, Girard S, Doualan J L, Thuau M, Moncorgé T and Tkachuk A M 2000 *Phys. Rev.* B **61** 5280
[2] Grzechnik A, Syassen K, Loa I, Hanfland M and Gesland J Y 2002 *Phys. Rev.* B **65** 104102
[3] Sen A, Chaplot L and Mittal R 2003 *Phys. Rev.* B **68** 134105
   Sen A, Chaplot L and Mittal R 2003 *Curr. Sci.* **85** 1045
[4] Li S, Ahuja R and Johansson B 2004 *J. Phys.: Condens. Matter* **16** S983
[5] Grzechnik A, Crichton W A, Hanfland M and van Smaalen S 2003 *J. Phys.: Condens. Matter* **15** 7261
[6] Hyde B G and Andersson S 1989 *Inorganic Crystal Structures* (New York: Wiley)
[7] Leger J M and Haines J 1997 *Eur. J. Solid State Inorg. Chem.* **34** 785
[8] Hammersley A P, Svensson S O, Hanfland M, Fitch A N and Häusermann D 1996 *High Pressure Res.* **14** 235
[9] Piermarini G J, Block S, Barnett J D and Forman R A 1975 *J. Appl. Phys.* **46** 2774
   Mao H K, Xu J and Bell P M 1986 *J. Geophys. Res.* **91** 4673
[10] Crichton W A and Mezouar M 2002 *High Temp. High Pressures* **34** 235
[11] Muller O and Roy R 1974 *The Major Ternary Structural Families* (Berlin: Springer)
[12] Boultif A and Louër D 1991 *J. Appl. Crystallogr.* **24** 987
[13] Laugier J and Bochu B *CHEKCELL* http://www.inpg.fr/LMGP
[14] Schlyter K 1952 *Ark. Kemi* **5** 73
   Otroshchenko L P, Aleksandrov B P, Maksimov B A and Simonov V I 1985 *Kristallografiya* **30** 658
[15] Kraus W and Nolze G 1998 *CPD Newsletter No. 20* International Union of Crystallography
[16] Wells A F 1984 *Structural Inorganic Chemistry* 5th edn (Oxford: Oxford University Press)
[17] Atavaeva E Y and Bendeliani N A 1979 *Inorg. Mater.* **15** 1487
[18] Cheetham A K, Fender B E F, Fuess H and Wright A F 1976 *Acta Crystallogr.* B **32** 94
   Kondratyuk I P, Krivandina E A and Sobolev B P 1988 *Kristallografiya* **33** 105
[19] Bendeliani N A 1984 *Inorg. Mater.* **20** 1489
[20] Dyuzheva T I, Lityagina L M, Demishev G B and Bendeliani N A 2002 *J. Alloys Compounds* **335** 59
   Dyuzheva T I, Lityagina L M, Demishev G B and Bendeliani N A 2003 *Inorg. Mater.* **39** 1198
[21] Trnovcová V, Fedorov P P, Barta C, Labas V, Meleshina V A and Sobolev B P 1999 *Solid State Ion.* **119** 173
[22] Fedorov P P, Buchinskaya I I, Bondareva O S, Bystrova A A, Vistin' L L, Ershov D A, Ivanov S P,
   Stasyuk V A and Sobolev B P 2000 *Russ. J. Inorg. Chem.* **45** 949
[23] Ranieri I M, Shimamura K, Nakano K, Fujita T, Courrol L C, Morato S P and Fukuda T 2000 *J. Cryst. Growth*
   217 145
[24] Grzechnik A, Crichton W A, Syassen K, Adler P and Mezouar M 2001 *Chem. Mater.* **13** 4255
[25] Dmitriev V, Sinitsyn V, Dilanian R, Machon D, Kuznetsov A, Ponyatovsky E, Lucazeau G and Weber H-P 2003
   J. Phys. Chem. Solids **64** 307
[26] Crichton W A, Aquilanti G, Grzechnik A and Pascarelli S 2004 *ESRF Experimental Report* HS-2100
   http://ftp.esrf.fr/pub/UserReports/25354_A.pdf
[27] Liu L 1979 *Earth Planet. Sci. Lett.* **44** 390
   Liu L 1982 *Earth Planet. Sci. Lett.* **57** 110
   Tange Y and Takahashi E 2004 *Phys. Earth Planet. Inter.* **143/144** 223
   Ono S, Funakoshi K, Nakajima Y, Tange Y and Katsura T 2004 *Contrib. Mineral. Petrol.* **147** 505
[28] Crichton W A, Parise J B, Antao S and Grzechnik A 2004 *Am. Mineral.* at press
[29] Errandonea D, Manjon F J, Somayazulu M and Häusermann D 2004 *J. Solid State Chem.* **177** 1087